



## Arsenic bioaccessibility in environmentally important arsenic minerals

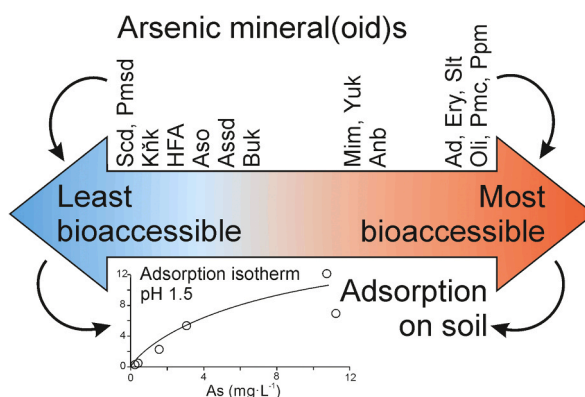
Petr Drahota<sup>\*</sup>, Vojtěch Ettler, Filip Košek

Institute of Geochemistry, Mineralogy and Mineral Resources, Faculty of Science, Charles University, Albertov 6, Prague 128 00, Czech Republic

### HIGHLIGHTS

- Arsenic bioaccessibility assessed in 16 arsenate and arsenic trioxide mineral (oid)s.
- Wide range of bioaccessibility from 0.15 % to 100 % under gastric conditions.
- Complete dissolution of Co, Cu, Pb, and Zn arsenates occurred in acidic conditions.
- Mineral solubility and soil retention capacity strongly affect As bioaccessibility.

### GRAPHICAL ABSTRACT



### ARTICLE INFO

**Keywords:**  
Arsenic  
Bioaccessibility  
Solubility  
Mineral(oid)s  
Soil

### ABSTRACT

The potential risk to humans from incidental ingestion of As-contaminated soil and mine waste is influenced by the mineralogical composition of the As phases present. Using the Solubility Bioaccessibility Research Consortium *in vitro* assay, simulating gastric conditions, we determined the oral bioaccessibility of As in 16 environmentally important As mineral(oid)s commonly found in mine waste and contaminated soils. Our results revealed a wide range of bioaccessibility values closely related to the solubility of the mineral(oid)s. Bioaccessibility values ranged from 0.15 % in minerals with great environmental stability such as scorodite and pharmacosiderite, to complete (100 %) release from minerals such as adamite, erythrite and pharmacolite. Intermediate bioaccessibility levels were observed in minerals such as arsenolite and yukonite, ranging from 6 % to 67 %. In mixtures with soil, the bioaccessibility of As in mineral(oid)s with low solubility was significantly reduced, with bioaccessibility values up to 8.7 times lower due to the effective adsorption of As by the soil. We conclude that the bioaccessibility of As in natural soil and mine waste is intricately influenced by both the mineralogical composition of As phases and the As retention capacity of natural materials under acidic conditions of gastric fluids.

<sup>\*</sup> Corresponding author.

E-mail address: [petr.drahota@natur.cuni.cz](mailto:petr.drahota@natur.cuni.cz) (P. Drahota).

## 1. Introduction

Arsenic (As) is a potentially carcinogenic metalloid that commonly occurs as a contaminant in mine wastes and soils affected by mining and ore processing operations. In areas affected by these activities, incidental oral ingestion and/or inhalation of dust from these materials often represent a primary exposure pathway of As, and the actual health risk depends on the bioaccessibility (soluble under gastrointestinal conditions) and therefore bioavailability of As (absorbed into the systematic circulation) in the ingested material [1,2]. Bioaccessibility is measured through several *in vitro* bioaccessibility (IVBA) assays that offer an inexpensive and expedient method simulating the dissolution of solid phase As in the gastrointestinal tract and have been validated by several animal model studies [3-5]. Estimating bioaccessibility from site-specific materials provides a realistic approximation of the relevant human exposure and, as such, is an important component of the health risk assessment.

Secondary arsenic minerals and mineraloids, the latter defined as X-ray amorphous natural phases with variable composition and structure, are among the most important scavengers of As in mine wastes and highly As-polluted soils [6,7]. The number of secondary arsenic mineral (oid)s is very high (nearly 520 arsenates and arsenites; [8]), but only a limited number of them have been repeatedly documented in mine wastes and soils [6,9]. These widespread As mineral(oid)s that can be considered ‘environmentally important’ phases are represented by stable and metastable arsenate and arsenic trioxide phases that vary significantly in stability and solubility [10]. Many studies have shown that the solubility of As mineral(oid)s is positively correlated with As bioavailability and bioaccessibility [11-15]. Arsenic minerals characterized by a notably low bioaccessibility comprise sparingly soluble sulfides and sulfosalts such as arsenopyrite (FeAsS), orpiment (As<sub>2</sub>S<sub>3</sub>), realgar (As<sub>4</sub>S<sub>4</sub>), arsenian pyrite (FeS<sub>2</sub>), and enargite (Cu<sub>3</sub>AsS<sub>4</sub>) [16-18, 13,19]. Crystalline and stable Fe(III) arsenates, such as scorodite (FeAsO<sub>4</sub>·2 H<sub>2</sub>O) and pharmacosiderite [KFe<sub>4</sub>(OH)<sub>4</sub>(AsO<sub>4</sub>)<sub>3</sub>·nH<sub>2</sub>O], were also reported to have very low bioaccessibility [17,18,20] due to their very low solubility [21,22]. Amorphous Fe(III) arsenate (HFA), As-bearing Fe(III) (oxyhydr)oxides (e.g., As sorbed to ferrihydrite [~Fe<sub>5</sub>HO<sub>8</sub>·4 H<sub>2</sub>O] or goethite [α-FeOOH]), or (hydroxy)sulfates (e.g., As incorporated into jarosite [KFe<sub>3</sub>(SO<sub>4</sub>)<sub>2</sub>(OH)<sub>6</sub>] or schwertmannite [Fe<sub>8</sub>O<sub>8</sub>(OH)<sub>6</sub>SO<sub>4</sub>]) increase bioaccessibility by more than an order of magnitude over sparingly soluble sulfides and crystalline Fe(III) arsenates [23,16,24,18,25]. Ehlert et al. [26] reported As bioaccessibilities of up to 7.3 % in synthetic HFA-ferrihydrite coprecipitates and found that bioaccessibility was strongly dependent on the mineralogical composition of the coprecipitate. Coprecipitates dominated by ferrihydrite exhibited lower bioaccessibility as a result of readsorption and/or surface precipitation of As released into the gastric solution. Additionally, Mikutta et al. [27] documented the precipitation of As-rich Fe (oxyhydr)oxides in gastric extracts during bioaccessibility testing of contaminated soils. In these tests, the bioaccessible As originating from As(V)-adsorbed ferrihydrite constituted 5–35 % of the total As content. Generally, higher bioaccessibilities of As were documented in samples where As was predominantly sequestered by naturally occurring jarosite or schwertmannite [16,18], while other studies have recommended the intentional formation of synthetic jarosite-group minerals, such as plumbojarosite and beudantite, to decrease the bioaccessibility of As in contaminated soils [28]. However, the highest bioaccessibility coincides with the presence of Ca-Fe arsenates such as arsenosiderite [Ca<sub>3</sub>Fe<sub>4</sub>(OH)<sub>6</sub>(AsO<sub>4</sub>)<sub>4</sub>·3 H<sub>2</sub>O] and yukonite [Ca<sub>2</sub>Fe<sub>3</sub>(AsO<sub>4</sub>)<sub>3</sub>(OH)<sub>4</sub>·4 H<sub>2</sub>O] [17,18,29], which are highly unstable under the low pH conditions of gastric solutions [30]. It is important to note that As mineralogy alone is not the sole physicochemical parameter influencing As bioaccessibility. Other factors, such as pH, organic matter content, Fe (oxyhydr)oxide mineralogy and content, texture, and redox conditions of soils and mine

waste, also play significant roles, as evidenced by notable differences in bioaccessibility values between samples with similar As mineral compositions [16,18,29]. For example, Fe content and speciation have been identified as significant explanatory variables dictating the heterogeneity of bioaccessibility results in natural samples ([14] and references therein). Yang et al. [31] reported a significant relationship between As (V) adsorption and Fe (oxyhydr)oxide content in soils, which generally reduces As bioaccessibility with increasing Fe content in natural samples. On the contrary, Fe complexation by glycine can promote the mobilization of As associated with Fe(III) mineral(oid) [32].

Although there is a widespread consensus that the bioaccessibility of As is closely associated with dominant secondary As-containing mineral (oid)s in mine waste and highly polluted soil [23,12,18,13,28,14], only a limited number of studies have investigated the bioaccessibility of As in pure phases or mineral systems. Beak et al. [33] and Ehlert et al. [26] investigated the bioaccessibility of As in amorphous coprecipitates of the HFA-ferrihydrite system, while Meunier et al. [17] reported the bioaccessibility of As in scorodite-rich and yukonite-rich materials. To date, no systematic study on the bioaccessibility of As in environmentally important As mineral(oid)s and its controlling factors has been conducted, despite its critical importance in understanding and evaluating the potential health risks associated with mine wastes and polluted soils. To address this research gap, we prepared and characterized sixteen As mineral(oid)s that are commonly encountered in mine wastes and highly polluted soils. While As-bearing phases like jarosite, schwertmannite, and Fe(III) (oxyhydr)oxides are commonly dominant in these environments, our study specifically focuses on environmentally important As mineral(oid)s where As is a primary stoichiometric component, such as arsenates and arsenic trioxide. By focusing on mineral(oid)s in which As is an integral part of the crystal structure, we aimed to directly assess As bioaccessibility in its most concentrated and environmentally significant natural phases.

We evaluated their As bioaccessibility using the Solubility Bioaccessibility Research Consortium gastric phase (SBRC-G) extraction test, which is now part of EPA’s Test Methods for Evaluating Solid Waste: Physical/Chemical Methods SW-846 as EPA Method 1340 [34]. This information was used to (i) provide comprehensive data on the bioaccessibility of As from environmentally important supergene As phases, which are essential for better understanding the bioaccessibility of As in complex natural samples, and (ii) determine potential factors influencing the varying levels of As bioaccessibility associated with these mineral(oid)s.

## 2. Materials and methods

### 2.1. Preparation and characterization of As mineral(oid)s

The samples selected for this study represent 16 environmentally important supergene arsenate and As trioxide mineral(oid)s. The synthetic analogues of adamite, annabergite, arsenosiderite, erythrite, mimetite, olivenite, pharmacosiderite, schultenite, scorodite and yukonite were prepared according to the well-established synthesis protocols [35-37,22,38,30,39-41] in the laboratory at the Charles University and University of Jena. A brief description of their syntheses and purification is outlined in the [Supplementary Information](#). An X-ray amorphous ferric arsenate (HFA), arsenolite, bukovskýite, kaňkite, pharmacolite, and picropharmacolite samples used here were natural, from the abandoned mining wastes and underground spaces near the municipality of Jáchymov (HFA, kaňkite, pharmacolite, and picropharmacolite) and Kutná Hora (bukovskýite) in the Czech Republic [42-44]. Arsenolite was obtained from the Arsenic Plant in the Tsumeb Smelter Complex, Namibia.

Total element contents (Al, As, Ca, Co, Fe, K, Mg, Na, Ni, P, Pb, S, Si, Zn) were determined in triplicate by inductively coupled plasma-optical

emission spectrometry (ICP-OES; Agilent 5100, USA) after acid digestion of the solids in 7 N HCl. Quality control samples were run every approximately 20 samples and consisted of blanks and certified solutions (NIST SRM 1643 f and 1640a). Values for certified solutions were within  $\pm 6\%$ .

Powder X-ray diffraction (XRD) and Raman spectrometry (RMS) were used to confirm the solid phases present. The XRD data were collected from 5 to 70° in 2theta using a X'Pert Pro diffractometer (PANalytical, the Netherlands) with a X'Celerator detector, Cu K $\alpha$  radiation (40 kV, 30 mA), 0.02° in 2theta step size, and 150 s dwell time/step. X'Pert High Score plus 3.0 software coupled with the ICDD PDF-2 database was used for analysis of the XRD patterns. The RMS measurements were performed using a Renishaw InVia Reflex Raman spectrometer (785 nm of a diode laser, laser power of 0.1–5%, translating into an output of 0.12–6 mW at the source, 20 s exposure accumulation, 10–20 accumulations).

## 2.2. Solid preparation and characterization for bioaccessibility determination

The reactivity of pure arsenic phases in the gastric conditions was studied in both composite quartz dust and soil dust samples. Quartz was chosen because it is a nonreactive material, ensuring that the results correspond specifically to the As bioaccessibility in As mineral(oid)s. However, considering the interaction that can occur between As and soil compounds, a soil mixture offers a more representative scenario for ingestion. The quartz sand (Sklopísek Střeleč, Czech Republic) and soil (Lufa Standard 2.2. soil, Lufa Speyer, Germany) were sieved to  $< 150\ \mu\text{m}$ , representing the particle size that is more adherent to human hands and thus more likely to be ingested [45]. Both composite quartz and soil samples were prepared by mixing  $475 \pm 3\ \text{mg}$  of quartz or soil dust with  $25.0 \pm 0.2\ \text{mg}$  of arsenic phase. Due to the limited quantity of the arsenic phases, surface area measurements of arsenic phases were not performed; however, the particle size was standardized to  $< 150\ \mu\text{m}$  to minimize variability in surface area effects on dissolution rates.

Major minerals of Lufa soil dust ( $< 150\ \mu\text{m}$ ) and its clay fraction were determined by XRD. The pH of the soil dust was measured in distilled water and 1 M KCl solution (soil-to-solution ratio (w/v) = 1:5) using a freshly calibrated glass electrode (SenTix® 41 electrode, WTW). Total sulfur (S), organic carbon (TOC), and inorganic carbon (TIC) were determined using an Eltra CS 530 and Eltra CS 500 TIC analyzers. Total element contents of soil dust were determined by ICP-OES after microwave-assisted digestion in mineral acids (HNO<sub>3</sub>, HF, and HClO<sub>4</sub>). The accuracy of the analytical determinations was checked by triplicate measurements of NIST SRM 2711a standard reference material and was found to be  $\leq 8\%$  of relative standard deviation for most elements (Table S1). Poorly crystalline metal-(oxyhydr)oxides with associated As in the soil and quartz dust were extracted in triplicate with 0.2 M ammonium-oxalate solution (solid-to-solution ratio (w/v) = 1:100, pH 3) for 2 h (100 rpm) in the dark [46]. To determine retention capacity for As(V) and As(III), single-point adsorption experiments were conducted in triplicate for soil and quartz dust. The experiments used a 0.1 M NaCl solution containing  $200\ \text{mg}\cdot\text{L}^{-1}$  As(V) (Na<sub>2</sub>HAsO<sub>4</sub>·7 H<sub>2</sub>O) or  $200\ \text{mg}\cdot\text{L}^{-1}$  As(III) (As<sub>2</sub>O<sub>3</sub>), with a solid-to-solution ratio (w/v) of 1:50. The tests were performed at pH 6.0 and pH 1.5, with equilibration times of 1 hour or 24 hours, 100 rpm and 37 °C. All extracts were analyzed by ICP-OES after 0.22- $\mu\text{m}$  filtration (Fisherbrand nylon membrane filters, Germany).

## 2.3. Bioaccessibility of arsenic

Arsenic bioaccessibility (IVBA<sub>As</sub>) was determined with EPA SW-846 Test Method 1340 [34] (also known as SBRC-G, Simplified Bioaccessibility Extraction Test or SBET), which has undergone inter- and intra-lab validation for predicting relative bioavailability (RBA<sub>As</sub>) in soil and for which As *in vitro* bioaccessibility data are strongly correlated

with mice and swine RBA [3,47]. EPA Method 1340 consists of one compartment representing the stomach in which mixture of glycine, HCl, and water simulates human stomach fluid at fasting pH [34,48]. The synthetic gastric fluid, prepared from N<sub>2</sub>-purged 0.4 M glycine solution (reagent-grade glycine in deionized water) adjusted to pH 1.5 with concentrated HCl (Suprapure grade, Merck), was added to solid samples in a liquid-to-solid ratio of 100 (v/w). The mixtures were gently rotated (80 rpm) at 37 °C for 1 h in a GFL 3032 incubator (GFL, Germany). The pH was regularly checked and manually adjusted by addition of HCl in case of any pH drift caused by the high buffering capacity of the samples (final pH =  $1.50 \pm 0.01$ ); at the end of incubation, the redox potential (E<sub>h</sub>; SenTix® ORP redox electrode, WTW) was measured. Subsequently, the suspensions were filtered through a 0.45- $\mu\text{m}$  nylon filter, diluted, and the filtrates were analyzed by ICP-OES. The bioaccessibility of As and Pb and extractability of metals (EX<sub>Metal</sub>; Ca, Co, Cu, Fe, K, Ni, Mg, S, and Zn) were expressed in g·kg<sup>-1</sup> and converted to their percentage of the total content. All extractions were performed at least in triplicate. A reference soil (NIST 2710a) was extracted in five replicates for quality control and the results (As bioaccessibility =  $32.0 \pm 0.8\%$ ; Pb bioaccessibility =  $53.5 \pm 0.9\%$ ;) were comparable with the ranges reported for an intra- and interlaboratory assessments for standard reference materials [49,50]. The surface and chemistry of HFA, arsenolite, and yukonite were evaluated before and after bioaccessibility testing using a TESCAN VEGA scanning electron microscope (SEM) equipped with an Oxford Link X-Max 50 energy-dispersive X-ray spectrometer (EDS).

Solubility curves for As mineral(oid), their saturation indices (SI), and the speciation of metal(loid)s in glycine extracts were calculated using PHREEQC software [51]. The LLNL and MINTEQ.V4 databases were augmented with the solubility products of the mineral(oid)s from the literature (Table S2).

## 3. Results and discussion

### 3.1. Elemental and mineralogical composition of mineral(oid)s and composite materials

Table 1 summarizes the elemental composition of all mineral(oid)s (complete data provided in Table S3). Arsenic and stoichiometric metal content (Ca, Co, Cu, Fe, Mg, Ni, Pb, Zn) of the mineral(oid)s ranged from 156 to 736 and from 31 to 741 g·kg<sup>-1</sup>, respectively. These concentrations correspond to 7800–36,800 mg·kg<sup>-1</sup> As in the composite samples, a range realistic for highly contaminated mine wastes [6,18]. Their chemical composition, as well as mineralogical characterization using XRD and RMS, indicate the purity and crystallinity of the phases, whether synthesized or collected from natural environments (Figure S1 and S2). The content of nonstoichiometric components was consistently lower than 23 g·kg<sup>-1</sup> (Table S3) and corresponded mainly to anions (PO<sub>4</sub><sup>3-</sup> and SO<sub>4</sub><sup>2-</sup>) incorporated into natural samples by substituting for AsO<sub>4</sub><sup>3-</sup> [52,53], or occasionally reflected the chemical composition of the reagents in the synthetic protocols (Na and SO<sub>4</sub><sup>2-</sup> in arseniosiderite, pharmacosiderite, and yukonite).

Quartz dust ( $< 150\ \mu\text{m}$ ) is a monomineralic material with very low amounts of metal (oxyhydr)oxides ( $\leq 27\ \text{mg}\cdot\text{kg}^{-1}$  of oxalate-extractable Fe, Al, or Mn), resulting in a negligible retention capacity for both As species (Table S4). Within the fine fraction of the Lufa soil ( $< 150\ \mu\text{m}$ ), quartz and organic matter are the predominant constituents, while minor minerals include K-feldspar, plagioclase, and clay minerals such as vermiculite and illite (Figure S3). The total concentration of As ( $16\ \text{mg}\cdot\text{kg}^{-1}$ ) and trace metals (Co, Cu, Ni, Pb, or Zn  $\leq 45\ \text{mg}\cdot\text{kg}^{-1}$ ) in soil is relatively low. The presence of organic matter, clay minerals, and metal-(oxyhydr)oxides (particularly Fe(III) (oxyhydr)oxides), as indicated by oxalate extractions ( $269\text{--}3470\ \text{mg}\cdot\text{kg}^{-1}$  of oxalate-extractable Fe, Al, or Mn), aligns with the elevated adsorption capacity of the soil for both As species (Table S4). Lufa soil dust generally sorbed more As (V) than As(III) at equivalent pH levels and equilibration times, likely

**Table 1**

Elemental composition of mineral(oid)s, their nominal formula, and molar metal/As ratio, As bioaccessibility (IVBA<sub>As</sub>), and metal extractability (EX<sub>Metal</sub>) for mineral(oid)s in the quartz dust or soil dust.

| Mineral(oid) <sup>a</sup>      |  | As                    | Metal <sup>c</sup>    | Metal/As                 | IVBA <sub>As</sub> | EX <sub>Metal</sub> | Metal/As                 | IVBA <sub>As</sub> | EX <sub>Metal</sub> | Metal/As                 |
|--------------------------------|--|-----------------------|-----------------------|--------------------------|--------------------|---------------------|--------------------------|--------------------|---------------------|--------------------------|
|                                |  | (g·kg <sup>-1</sup> ) | (g·kg <sup>-1</sup> ) | (mol·mol <sup>-1</sup> ) | Quartz dust        |                     | (mol·mol <sup>-1</sup> ) | Soil dust          |                     | (mol·mol <sup>-1</sup> ) |
|                                |  |                       |                       |                          | (%)                | (%)                 |                          | (%)                | (%)                 |                          |
| Scorodite                      | FeAsO <sub>4</sub> ·2 H <sub>2</sub> O   | 342                   | 253                   | 0.99                     | 0.15               | 0.14                | 0.92                     | 0.07               | —                   | —                        |
| Pharmacosiderite               | KFe <sub>4</sub> (OH) <sub>4</sub> (AsO <sub>4</sub> ) <sub>3</sub> ·nH <sub>2</sub> O                     | 273                   | 274                   | 1.34                     | 0.30               | 0.26                | 1.18                     | 0.09               | —                   | —                        |
| Kaňkite <sup>b</sup>           | FeAsO <sub>4</sub> ·3.5 H <sub>2</sub> O   | 289                   | 218                   | 1.01                     | 1.1                | 1.1                 | 0.98                     | 0.33               | —                   | —                        |
| HFA <sup>b</sup>               | FeAsO <sub>4</sub> ·nH <sub>2</sub> O  | 220                   | 233                   | 1.42                     | 2.8                | 2.7                 | 1.39                     | 0.33               | —                   | —                        |
| Arsenolite <sup>b</sup>        | As <sub>2</sub> O <sub>3</sub>   | 736                   | —                     | —                        | 5.9                | —                   | —                        | 1.3                | —                   | —                        |
| Arseniosiderite                | Ca <sub>3</sub> Fe <sub>4</sub> (OH) <sub>6</sub> (AsO <sub>4</sub> ) <sub>4</sub> ·3 H <sub>2</sub> O     | 296                   | 211                   | 0.96                     | 7.5                | 5.7                 | 0.73                     | 5.1                | —                   | —                        |
| Bukovskýite <sup>b</sup>       | Fe <sub>2</sub> (AsO <sub>4</sub> )(SO <sub>4</sub> )(OH)·9 H <sub>2</sub> O                               | 177                   | 247                   | 1.87                     | 12                 | 16                  | 2.44                     | 5.5                | 8.3 <sup>d</sup>    | 2.79 <sup>d</sup>        |
| Mimetite                       | Pb <sub>5</sub> (AsO <sub>4</sub> ) <sub>3</sub> Cl  | 159                   | 741                   | 1.69                     | 59                 | 60                  | 1.71                     | 63                 | 66                  | 1.77                     |
| Yukonite                       | Ca <sub>2</sub> Fe <sub>3</sub> (OH) <sub>4</sub> (AsO <sub>4</sub> ) <sub>3</sub> ·4 H <sub>2</sub> O     | 273                   | 181                   | 0.89                     | 68                 | 59                  | 0.77                     | 60                 | 43 <sup>d</sup>     | 0.64 <sup>d</sup>        |
| Annabergite                    | Ni <sub>3</sub> (AsO <sub>4</sub> ) <sub>2</sub> ·8 H <sub>2</sub> O                                       | 257                   | 317                   | 1.57                     | 67                 | 64                  | 1.52                     | 58                 | 58                  | 1.55                     |
| Adamite                        | Zn <sub>2</sub> (AsO <sub>4</sub> )(OH)  | 278                   | 468                   | 1.93                     | 98                 | 97                  | 1.91                     | 87                 | 87                  | 1.93                     |
| Erythrite                      | Co <sub>3</sub> (AsO <sub>4</sub> ) <sub>2</sub> ·8 H <sub>2</sub> O                                       | 256                   | 336                   | 1.67                     | 94                 | 95                  | 1.49                     | 92                 | 95                  | 1.55                     |
| Schultenite                    | Pb(AsO <sub>3</sub> OH)  | 156                   | 444                   | 1.03                     | 101                | 98                  | 1.00                     | 102                | 103                 | 1.05                     |
| Olivenite                      | Cu <sub>2</sub> (AsO <sub>4</sub> )(OH)  | 211                   | 339                   | 1.89                     | 100                | 101                 | 1.90                     | 104                | 106                 | 1.92                     |
| Picropharmacolite <sup>b</sup> | Ca <sub>4</sub> Mg(AsO <sub>3</sub> OH) <sub>2</sub> (AsO <sub>4</sub> ) <sub>2</sub> ·11 H <sub>2</sub> O | 331                   | 153                   | 0.86                     | 99                 | 102                 | 0.89                     | 97                 | 99 <sup>d</sup>     | 0.88 <sup>d</sup>        |
| Pharmacolite <sup>b</sup>      | Ca(AsO <sub>3</sub> OH)·2 H <sub>2</sub> O   | 362                   | 180                   | 0.93                     | 100                | 102                 | 0.95                     | 92                 | 93 <sup>d</sup>     | 0.93 <sup>d</sup>        |

<sup>a</sup> Arsenic mineral(oid)s are listed in order of their increasing As bioaccessibility.

<sup>b</sup> The mineral(oid)s denote natural origin, while the remaining are synthetic.

<sup>c</sup> Metals are represented by Fe, Pb, Ni, Zn, Co, Cu, or Ca, with a preference for Fe, when mineral(oid) contains two metals.

<sup>d</sup> The extractability of Fe or Ca was calculated by subtracting the extractability in pure soil from that in the mixture of soil and As mineral.

due to the stronger electrostatic interactions or inner-sphere complexation of As(V) species with positively charged surface sites. The retention capacity was higher at pH 1.5 than at pH 6, consistent with other studies demonstrating a decrease in As(V) and often in As(III) sorption with increasing pH [54,55], which can be attributed to the higher positive surface charge at lower pH. Despite the incomplete retention of As species in 1 hour (25–90 % sequestered within 24 hours), our data show that the soil can adsorb 730 mg·kg<sup>-1</sup> As(V) and 180 mg·kg<sup>-1</sup> As(III) under the conditions of the IVBA assay (1 hour, pH 1.5, and 37 °C).

### 3.2. Arsenic bioaccessibility and metal extractability in mineral(oid)s

The bioaccessible As concentration measured for the mineral(oid)s in the quartz dust ranged from 0.5 to 363 g·kg<sup>-1</sup> (Table S5). These values indicate that the IVBA<sub>As</sub> in the mineral(oid)s are highly variable, ranging from 0.15 % to 101 % (Table 1). The measured bioaccessible Pb and extractable metal (Co, Cu, Fe, Ni, or Zn) concentrations ranged from 0.4 to 441 g·kg<sup>-1</sup> (Table S5), with corresponding IVBA<sub>Pb</sub> and EX<sub>Metal</sub> ranging from 0.14 % to 102 % (Table 1). The latter values are similar to the IVBA<sub>As</sub>, with a mean percentage difference of 2.2 %. The paired *t*-test (*p* = 0.479) and Wilcoxon signed-rank test (*p* = 0.418) indicate no significant difference between the IVBA<sub>As</sub> and corresponding IVBA<sub>Pb</sub> or EX<sub>Metal</sub>, with variations ranging from -13.2 to 7.6 %.

Based on their IVBA<sub>As,Pb</sub> and EX<sub>Metal</sub> levels, the mineral(oid)s can be classified into five groups. Scorodite and pharmacosiderite are almost insoluble minerals in gastric solution, with IVBA<sub>As</sub> ≤ 0.3 %. Kaňkite and HFA exhibit relatively low IVBA<sub>As</sub> (1–3 %), while arsenolite, arseniosiderite, and bukovskýite display moderate IVBA<sub>As</sub> (6–12 %). High IVBA<sub>As</sub> (59–67 %) are found in mimetite, yukonite, and annabergite. The remaining As minerals, including adamite, erythrite, schultenite, olivenite, pharmacolite, and picropharmacolite are completely soluble in the simulated gastric solution (Table 1). These values are generally consistent with limited IVBA<sub>As</sub> values reported for pure phases in the literature. Specifically, they correspond to the IVBA<sub>As</sub> values of 2.9–7.3 % for HFA-rich coprecipitates [26], but are higher than those found for scorodite-rich (0.03–0.08 %) and yukonite-rich (10–19 %) materials [17]. This difference may stem from the different methodological conditions of the PBET assay (pH<sub>Gastric</sub> = 1.8; absence of glycine) used by Meunier et al. [17], as well as the composite nature of their samples.

The arsenic mineralogy is not the only factor influencing the IVBA<sub>As</sub> of composite materials, but it often plays a significant or even exclusive role. Arsenic bioaccessibility documented for composite samples of mine wastes and mining-impacted soils with defined arsenic mineralogy spans a wide range, with values between 0.3 % and 90 % [56,18,29,20,19]. In accordance with our results, the lowest IVBA<sub>As</sub> (≤0.6 %) were documented in samples, where scorodite was confirmed as the only dominant As-bearing mineral [18,20]. However, the As mineralogy of mine waste and soil samples is usually more complex with scorodite commonly associated with metastable ferric arsenates such as HFA and kaňkite, as well as As-bearing Fe(III) (oxyhydr)oxides and (hydroxy)sulfates such as ferrihydrite, goethite, jarosite, and schwertmannite [6]. The co-occurrence of these more reactive mineral(oid)s with less reactive scorodite or pharmacosiderite increased IVBA<sub>As</sub> of composite materials to values ranging from 2.5 % to 41 % [18,20,19]. Such a wide range of percentages cannot be easily related to the relative abundance of As mineral(oid)s with variable reactivity, as shown in the results of Meunier et al. [18] and Whitacre et al. [19]. This discrepancy suggests that other factors influence the varying IVBA<sub>As</sub> of natural samples with complex As mineralogy. These factors likely include differences in the availability of mineral surfaces for dissolution reactions and the presence of minor to rare, highly reactive As phases. The availability of mineral surfaces is critical for dissolution, and the specific surface area of As mineral(oid)s should be considered. This is particularly important when comparing the dissolution behavior of synthetic and natural phases, as differences in crystallinity can lead to variations in the surface area of each phase (see [21]). Although we were unable to measure the specific surface area of As mineral(oid)s in our study due to limited sample quantities, their crystallinity can be indicated by their XRD patterns (Fig. S1). To minimize variability related to particle size effects, all samples were powdered and sieved to a uniform particle size of < 150 μm, ensuring consistency in surface area-to-volume ratios among the samples. The presence of minor, highly reactive As phases may also help explain the discrepancy between lower IVBA<sub>As</sub> observed in pure arsenolite (6 %; Table 1) and higher values found in arsenolite-rich smelter dust samples (35–77 %) from Tsumeb (Namibia) [56]. The notably higher As bioaccessibility in the smelter dust may be attributed to the presence of minor Al, Cu, and Pb arsenate phases such as alarsite (AlAsO<sub>4</sub>), conichalcite [CaCu(AsO<sub>4</sub>)(OH)], johnbaumite [Ca<sub>5</sub>(AsO<sub>4</sub>)<sub>3</sub>(OH)], and mimetite [57]. Unlike arsenolite, Cu and Pb arsenates

were not detected in the extraction residues of the smelter dust [56], corroborating our findings of their complete solubility in the gastric solutions (Table 1). However, Co, Cu, Pb, and Zn arsenates almost always occur as minor or rare As minerals in mining-impacted materials [6]. Consequently, the highest  $IVBA_{As}$  (19–90 %) were documented in materials, where As is predominantly bound to Ca-Fe arsenates such as arseniosiderite and yukonite [18,29]. The wide range of  $IVBA_{As}$  (19–90 %) in their samples cannot be solely explained by the variable distribution of arseniosiderite and yukonite in the samples, which display different As bioaccessibility (Table 1), but reach a maximum of only 70 % (yukonite). It is possible that the higher  $IVBA_{As}$  ( $\leq 90$  %) in natural samples from the gold mining region of Victoria (Australia) could be attributed to the minor presence of soluble As phases, such as Ca and Mg arsenates, which are expected in high-pH environments rich in Ca or Mg [44], similar to those found in the natural samples. Another contributing factor may be the increased dissolution kinetics of Ca-Fe arsenates in these natural samples, potentially due to a greater surface availability or the different crystallographic nature of the natural minerals compared to synthetic ones.

### 3.3. Controls on arsenic bioaccessibility in mineral(oid)s

Numerous studies have indicated that the bioaccessibility of As mineral(oid)s is closely linked to their solubility [11–14]. Calculated solubility of the mineral(oid)s showed a strong pH-dependance (Fig. 1) and indicated that, independently of the quality of the available thermodynamic data, the solubility order at pH 1.5 generally corresponds to  $IVBA_{As}$  (Table 1). At this pH, scorodite exhibits the lowest solubility and similar or even lower solubility can be expected for pharmacosiderite, which shows no signs of dissolution in 5 N HCl, even after one day [22]. According to the  $IVBA_{As}$  values, the minerals with high solubility include Ni, Co, Cu and Zn arsenates, while Ca and Ca-Mg arsenates are the most soluble minerals (Fig. 1). Although the  $IVBA_{As}$  of several minerals slightly deviated from the solubility predictions, schultenite and arsenolite showed the most significant differences; schultenite dissolved readily, while arsenolite exhibited limited solubility in gastric solution. The latter phenomenon can be ascribed to a slow dissolution of arsenolite. It is important to note that the solubility results in Fig. 1 reflect equilibrium conditions, whereas the 1-hour bioaccessibility test is

likely far from reaching equilibrium for arsenolite. In fact, laboratory experiments with arsenolite dissolution reported that the system may reach equilibrium after several months or perhaps even after a year [58]. This slow dissolution process suggests that the limited solubility observed in short-term bioaccessibility tests may not fully reflect long-term behavior of arsenolite under equilibrium conditions. The explanation for the high level of  $IVBA_{As}$  in schultenite is not clear. However, thermodynamic data for schultenite, determined from a solubility study on a natural sample [59], could be problematic because the authors did not provide any chemical analyses, proof of homogeneity, or evidence ruling out microscopic impurities.

To assess the potential for As precipitation in the glycine extract, saturation indices for As-bearing phases were calculated. The results indicate an undersaturation for all investigated As mineral(oid)s ( $SI \leq -1.5$ ) and for all other As-bearing phases ( $SI \leq -2.1$ ), including Fe(III) (oxyhydr)oxides. Saturation was observed only for scorodite ( $SI = +0.1$ ) in the yukonite sample, but its formation is unlikely during a 1-h extraction at 37 °C and pH 1.5 [60]. This suggests that homogenous As precipitation did not influence the  $IVBA_{As}$  in the studied mineral(oid)s. It should be noted that the mobilization of As from mineral(oid)s is facilitated by the formation of glycine complexes with cationic species [61,62]. Speciation modeling indicates that 84–97 % Fe(III) and up to 27 % Ca are stabilized in the solution through the formation of  $[FeHGly]^{3+}$  and  $[CaHGly]^{2+}$  complexes, respectively. The ability of glycine to complex with these cations enhances the dissolution of Fe- and Ca-bearing As mineral(oid)s. In contrast, the complexation of other metals by glycine is low (4 % for Cu) or negligible (Co, Mg, Ni, Pb, and Zn). Consequently, glycine may result in higher  $IVBA_{As}$  in these phases compared to IVBA assays without glycine [32]. This highlights the importance of glycine in simulating gastrointestinal conditions, as its presence can increase the bioaccessibility of As, particularly in complex environmental samples containing Fe (oxyhydr)oxides. However, glycine is not the only factor influencing the dissolution of As phases in IVBA assays. For example, soluble phosphate, present in the gastrointestinal system, can both desorb As from Fe (oxyhydr)oxides [63,64] and promote the dissolution of arsenates such as HFA and yukonite [53]. Similarly, reducing agents like ascorbic acid or pepsin, naturally secreted in the stomach, lower the redox potential of gastric solutions and may facilitate the dissolution of As-bearing Fe phases [11,24]. These

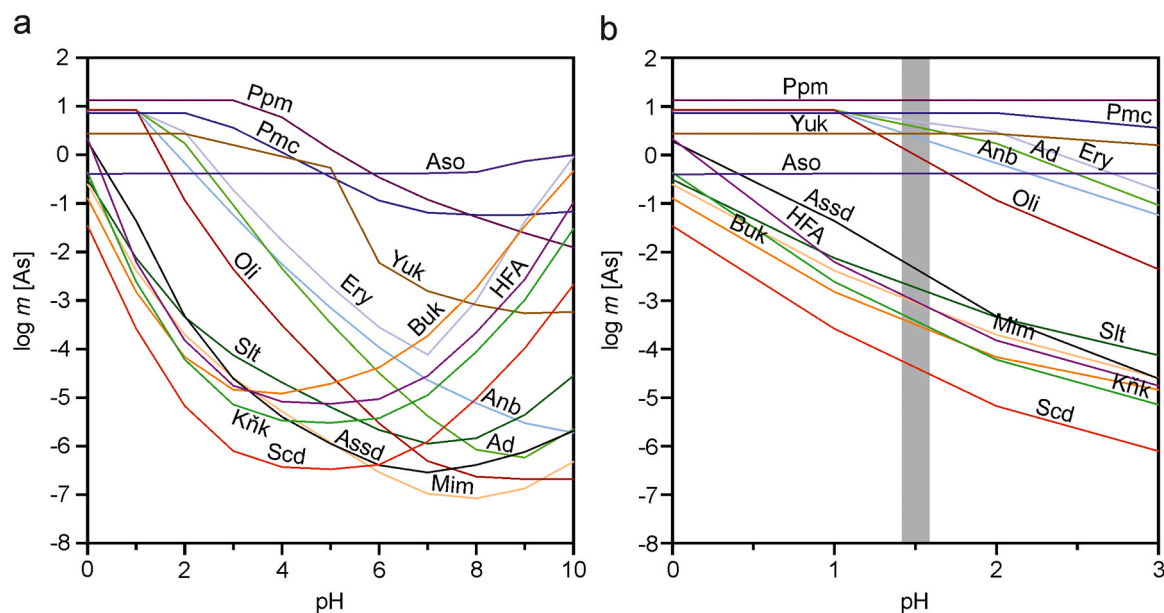


Fig. 1. Calculated solubility for the arsenic mineral(oid)s. Mineral abbreviations: adamite (Ad), amorphous ferric arsenate (HFA), annabergite (Anb), arseniosiderite (Assd), arsenolite (Aso), bukovskýite (Buk), erythrite (Ery), kańkite (Kńk), mimetite (Mim), olivenite (Oli), pharmacolite (Pmc), picropharmacolite (Ppm), schultenite (Slt), scorodite (Scd), yukonite (Yuk).

and other differences in IVBA operational parameters can lead to varying IVBA<sub>As</sub> values for the same samples, highlighting the need to consider multiple physiological factors when assessing As bioaccessibility and exposure risks.

The molar metal/As ratios in the extracts were quite similar to the molar metal/As ratios in the solids (Table 1), indicating a congruent dissolution of the mineral(oid)s in the glycine solution. Fig. 2 illustrates the relationship between the molar metal/As in the extract and the metal/As in the solids for all mineral(oid)s in both the quartz and soil composite samples. Nearly all solids dissolved congruently in both sample types, displaying similar releases of metal and As, with the exception of several complex Fe arsenates, where the congruence was less pronounced. Specifically, Ca-Fe arsenates (arsenosiderite and yukonite) with lower Fe/As in the solids exhibited a slightly higher release of As compared to Fe, while bukovskýite (high Fe/As ratio in the solid) released more Fe than As (Fig. 2). A comparable trend, with significantly higher variations in the molar ratios, was observed for HFA-ferrihydrite coprecipitates and was attributed to As readsorption and/or surface precipitation at higher Fe/As solid ratios [26]. Ehlert et al. [26] reported an incongruent dissolution of HFA-ferrihydrite coprecipitates, but also showed that increasing the liquid-to-solid ratios from 100 to 5000 leads to a congruent dissolution. Consistent with their findings, our liquid-to-mineral(oid) ratio of 2000:1 was sufficiently high to ensure congruent or near-congruent dissolution in the bioaccessibility testing of pure As mineral(oid)s.

### 3.4. Effect of soil on arsenic bioaccessibility in mineral(oid)s

The bioaccessible As concentration measured for mineral(oid)s in soil dust ranged from 0.2 to 334 g·kg<sup>-1</sup>, with the corresponding values of IVBA<sub>As</sub> between 0.07 % and 104 % (Table 1 and S5). The calculated values of IVBA<sub>Pb</sub> and EX<sub>Metal</sub> were nearly identical to the IVBA<sub>As</sub> values for most mineral(oid)s where these calculations were possible (for minerals with EX<sub>Metal</sub> ≥ bukovskýite, Table 1). This indicates congruent or near-congruent dissolution of these minerals in the soil dust, similar to the congruent dissolution observed in quartz dust (Fig. 2). On the basis of the IVBA<sub>As,Pb</sub> and EX<sub>Metal</sub> values, the mineral(oid)s could be categorized in a manner similar to quartz dust samples. However, the IVBA<sub>As</sub> values for many mineral(oid)s in soil dust are considerably lower than those found in quartz dust samples (Table 1). While the soluble minerals (adamite, erythrite, schultenite, olivenite, pharmacolite, and picroparmacolite) in the quartz dust samples dissolved almost completely in the soil samples, three previously defined groups of mineral(oid)s with the lowest solubility in the glycine solution exhibited significantly lower IVBA<sub>As</sub> in the soil dust. Specifically, scorodite and

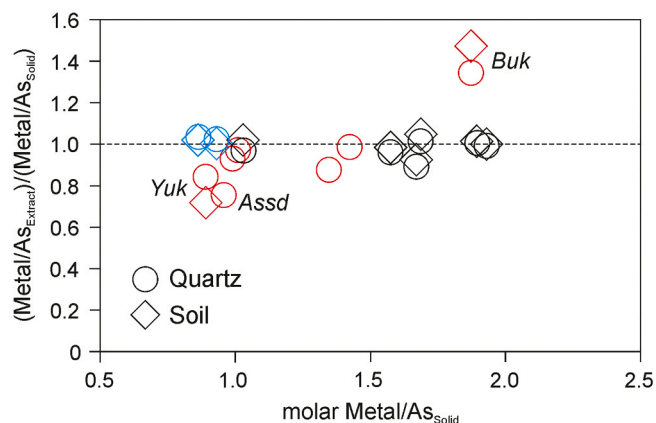


Fig. 2. Relative changes in the molar Metal/As<sub>Extract</sub> ratio with increasing molar Metal/As<sub>Solid</sub> ratio. Metals include Co, Cu, Ni, Zn (black symbols), Fe (red symbols), or Ca (blue symbols). The dashed line indicates the line of congruent dissolution. Arsenosiderite (Assd), bukovskýite (Buk), yukonite (Yuk).

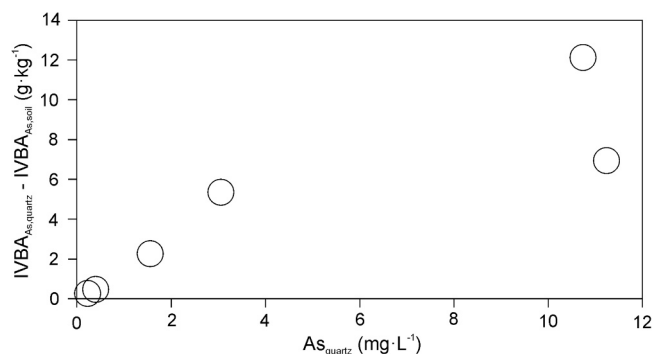


Fig. 3. Relationship between the difference of bioaccessible As concentrations in quartz (IVBA<sub>As,quartz</sub>) and soil dust (IVBA<sub>As,soil</sub>) and the dissolved As concentration in the quartz dust (As<sub>quartz</sub>) for scorodite, pharmacosiderite, kaňkite, HFA, arsenosiderite, and bukovskýite.

pharmacosiderite showed IVBA<sub>As</sub> lower than 0.1 %; kaňkite and HFA displayed IVBA<sub>As</sub> of 0.3 %, and the minerals with moderate IVBA<sub>As</sub> (arsenolite, arsenosiderite, and bukovskýite) exhibited values between 1.3 % and 5.5 % (Table 1). These IVBA<sub>As</sub> values are 1.5–8.7 times lower than those for the corresponding mineral(oid)s in the quartz dust samples, exhibiting a general trend of decreasing differences as bioaccessible As concentrations increase. These findings are consistent with the sequestration of As by the soil. In agreement with our results, the retention capacity of the Lufa soil, estimated at 730 mg·kg<sup>-1</sup> As(V) and 180 mg·kg<sup>-1</sup> As(III) (Table S4), indicates negligible relative sequestration of As(V) (<8 %) released from highly soluble phases such as yukonite and other more soluble minerals listed in Table 1. This reflects the fact that the amount of As released from these highly soluble minerals far exceeds the retention capacity of the soil. In contrast, the low IVBA<sub>As</sub> values for scorodite, pharmacosiderite, kaňkite, HFA, arsenosiderite, and bukovskýite in soil mixtures can be completely attributed to the adsorption of As onto soil sorbents. Here, the increasing amount of adsorbed As increases with bioaccessible As concentrations in the mineral(oid)s (Fig. 3), likely reflecting the adsorption isotherm of As(V) in soils [54,55].

Another aspect that could potentially reduce the bioaccessibility of As and was tested in our mixed samples is the mechanical barrier on the surface of As mineral(oid)s caused by the trapping of soil particles. Unlike the quartz samples, the surface of HFA and yukonite after bioaccessibility extractions in soil samples revealed the presence of aluminosilicate particles (Figure S4a,b), which, however, covered only a small portion of mineral(oid) surfaces and therefore likely did not play a significant role in reducing bioaccessibility values in soils. The absence of aluminosilicate cover on arsenolite surfaces (Figure S4c) suggests that the large difference between the bioaccessibility of As in quartz and soil samples, which cannot be completely attributed to As(III) sorption in soil, may be caused by other factors related to the very slow oxidation and dissolution of this mineral in the soil environment [58].

## 4. Conclusion

In the study, we investigated As bioaccessibility in 16 environmentally important supergene arsenate and As trioxide mineral(oid)s. Bioaccessibility varied widely (0.15–100 %), driven primarily by the differential solubility of the mineral(oid)s under acidic gastric conditions. Stable and crystalline phases (e.g., scorodite, pharmacosiderite) exhibited low IVBA<sub>As</sub>, while less crystalline or metastable phases (e.g., HFA, kaňkite, yukonite) showed higher IVBA<sub>As</sub>. The highest bioaccessibility was observed in minerals stable under alkaline conditions, such as Ca and Ca-Mg arsenates, and arsenates of Cu, Co, Ni, Pb, and Zn.

Bioaccessibility in soil mixtures was frequently lower than in quartz dust due to the retention of As released by soil sorbents, highlighting the

influence of sorption capacity on IVBA<sub>As</sub> in natural samples. These results emphasize the importance of considering both mineral(oid) composition and sorption capacity when assessing As exposure risks in contaminated soils and mine wastes. When integrated with site-specific bioaccessibility measurements, our findings contribute to a deeper understanding of the potential health risks associated with exposure to As in contaminated soils and mine waste.

### Environmental Implications

This study demonstrates that arsenic bioaccessibility varies significantly (0.15–100 %) among 16 arsenate and arsenic trioxide mineral (oid)s, commonly found in contaminated soils and mine waste. A novel finding is that arsenic bioaccessibility is primarily controlled by the mineralogy of these phases, which relates to their solubility, and the retention capacity of the surrounding materials, such as soil and waste. These insights emphasize the need for targeted remediation strategies that consider both mineral composition and soil retention to effectively mitigate arsenic exposure risks in contaminated environments.

### CRedit authorship contribution statement

**Petr Drahota:** Writing – original draft, Visualization, Validation, Methodology, Investigation, Funding acquisition, Formal analysis, Conceptualization. **Vojtěch Ettler:** Writing – review & editing, Visualization, Investigation, Funding acquisition, Formal analysis. **Filip Košek:** Writing – review & editing, Visualization, Investigation, Formal analysis.

### Declaration of Competing Interest

The authors declare that they have no known competing financial interests or personal relationships that could have appeared to influence the work reported in this paper.

### Acknowledgement

This study was supported by the Czech Science Foundation (GAČR 22–27939S) and the Johannes Amos Comenius Programme (P JAC), project No. CZ.02.01.01/00/22\_008/0004605, Natural and anthropogenic georisks. We thank numerous colleagues for their support in the laboratories (Marie Fayadová, Lenka Jílková, Věra Vonásková) and Juraj Majzlan (University of Jena) for the sample of synthetic and purified pharmacosiderite.

### Appendix A. Supporting information

Supplementary data associated with this article can be found in the online version at [doi:10.1016/j.jhazmat.2024.136838](https://doi.org/10.1016/j.jhazmat.2024.136838).

### Data availability

The data are available on the zenodo portal ([doi:10.5281/zenodo.14235210](https://doi.org/10.5281/zenodo.14235210)).

### References

- Bradham, K.D., Diamond, G.L., Burgess, M., Juhasz, A., Klotzbach, J.M., Maddaloni, M., Nelson, C., Scheckel, K., Serda, S.M., Stifelman, M., Thomas, D.J., 2018. In vivo and in vitro methods for evaluating soil arsenic bioavailability: relevant to human health risk assessment. *J Toxicol Environ Health B Crit Rev* 2, 83–114. <https://doi.org/10.1080/10937404.2018.1440902>.
- Denys, S., Caboche, J., Tack, K., Rychen, G., Wragg, J., Cave, M., Jondreville, C., Feidt, C., 2012. In vivo validation of the unified BARGE method to assess the bioaccessibility of arsenic, antimony, cadmium, and lead in soils. *Environ Sci Technol* 46, 6252–6260. <https://doi.org/10.1021/es3006942>.
- Bradham, K.D., Nelson, C., Juhasz, A.L., Smith, E., Scheckel, K., Obenour, D.R., Miller, B.W., Thomas, D.J., 2015. Independent data validation of an in vitro method for the prediction of the relative bioavailability of arsenic in contaminated soils. *Environ Sci Technol* 49, 6312–6318. <https://doi.org/10.1021/acs.est.5b00905>.
- Juhasz, A.L., Herde, P., Herde, C., Boland, J., Smith, E., 2014. Validation of the predictive capabilities of the Sbrc-G in vitro assay for estimating arsenic relative bioavailability in contaminated soils. *Environ Sci Technol* 48, 12962–12969. <https://doi.org/10.1021/es503695g>.
- Rodriguez, R.R., Basta, N.T., Casteel, S.W., Pace, L.W., 1999. An in vitro gastrointestinal method to estimate bioavailable arsenic in contaminated soils and solid media. *Environ Sci Technol* 33, 642–649. <https://doi.org/10.1021/es980631h>.
- Majzlan, J., Drahota, P., Filippi, M., 2014. Parageneses and crystal chemistry of arsenic minerals. *Rev Mineral Geochem* 79, 17–184. <https://doi.org/10.2138/rmg.2014.79.2>.
- Morin, G., Calas, G., 2006. Arsenic in soils, mine tailings, and former industrial sites. *Elements* 2, 97–101. <https://doi.org/10.2113/gselements.2.2.97>.
- IMA, 2024. The new IMA List of Minerals – A Work in Progress – Updated March 2024. ([http://efaidnbmnnnibpajpcgiclfefndmkaj/http://cnmnc.units.it/master\\_list/IMA\\_Master\\_List\\_%282024-03%29.pdf](http://efaidnbmnnnibpajpcgiclfefndmkaj/http://cnmnc.units.it/master_list/IMA_Master_List_%282024-03%29.pdf)).
- Drahota, P., Filippi, M., 2009. Secondary arsenic minerals in the environment: A review. *Environ Int* 35, 1243–1255. <https://doi.org/10.1016/j.envint.2009.07.004>.
- Nordstrom, D.K., Majzlan, J., Königsberger, E., 2014. Thermodynamic properties for arsenic minerals and aqueous species. *Rev Mineral Geochem* 79, 217–255. <https://doi.org/10.2138/rmg.2014.79.4>.
- Basta, N.T., Juhasz, A., 2014. Using *in vivo* bioavailability and/or *in vitro* gastrointestinal bioaccessibility testing to adjust human exposure to arsenic from soil ingestion. *Rev Mineral Geochem* 79, 451–472. <https://doi.org/10.2138/rmg.2014.79.9>.
- Davis, A., Ruby, M.V., Bloom, M., Schoof, R., Freeman, G., Bergstrom, P.D., 1996. Mineralogical constraints on the bioavailability of arsenic in smelter-impacted soils. *Environ Sci Technol* 30, 392–399. <https://doi.org/10.1021/es9407857>.
- Ruby, M.V., Schoof, R., Brattin, W., Goldade, M., Post, G., Harnois, M., Mosby, D. E., Casteel, S.W., Berti, W., Carpenter, M., Edwards, D., Cragin, D., Chappell, W., 1999. Advances in evaluating the oral bioavailability of inorganics in soil for use in human health risk assessment. *Environ Sci Technol* 33, 3697–3705. <https://doi.org/10.1021/es990479z>.
- Sowers, T.D., Nelson, C.M., Blackmon, M.D., Jerden, M.L., Kirby, A.M., Diamond, G.L., Bradham, K.D., 2022. Interconnected soil iron and arsenic speciation effects on arsenic bioaccessibility and bioavailability: a scoping review. *J Toxicol Environ Health* 25, 1–22. <https://doi.org/10.1080/10937404.2021.1996499>.
- Stevens, B.N., Betts, A.R., Miller, B.W., Scheckel, K.G., Anderson, R.H., Bradham, K.D., Casteel, S.W., Thomas, D.J., Basta, N.T., 2018. Arsenic speciation of contaminated soils/solid wastes and relative oral bioavailability in swine and mice. *Soil Syst* 2, 1–27. <https://doi.org/10.3390/soilsystems2020027>.
- Karna, R.R., Noerpel, M., Betts, A.R., Scheckel, K.G., 2017. Lead and arsenic bioaccessibility and speciation as a function of soil particle size. *J Environ Qual* 23, 1225–1235. <https://doi.org/10.2134/jeq2016.10.0387>.
- Meunier, K., Koch, I., Reimer, K.J., 2011. Effects of dissolution kinetics on bioaccessible arsenic from tailings and soils. *Chemosphere* 84, 1378–1385. <https://doi.org/10.1016/j.chemosphere.2011.05.019>.
- Meunier, L., Walker, S.R., Wragg, J., Parsons, M.B., Koch, I., Jamieson, H.E., Reimer, K.J., 2010. Effects of soil composition and mineralogy on the bioaccessibility of arsenic from tailings and soil in gold mine district of Nova Scotia. *Environ Sci Technol* 44, 2667–2674. <https://doi.org/10.1021/es9035682>.
- Whitacre, S., Basta, N., Stevens, B., Hanley, V., Anderson, R., Scheckel, K., 2017. Modification of an existing in vitro method to predict relative bioavailable arsenic in soils. *Chemosphere* 180, 545–552. <https://doi.org/10.1016/j.chemosphere.2017.03.134>.
- Toujaguez, R., Ono, F.B., Martins, V., Cabrera, P.P., Blanco, A.V., Bundschuh, J., Guilherme, L.R.G., 2013. Arsenic bioaccessibility in gold mine tailings of Delita, Cuba. *J Hazard Mater* 262, 1004–1013. <https://doi.org/10.1016/j.jhazmat.2013.01.045>.
- Langmuir, D., Mahoney, J., Rowsdon, J., 2006. Solubility products of amorphous ferric arsenate and crystalline scorodite (FeAsO<sub>4</sub>·2H<sub>2</sub>O) and their application to arsenic behavior in buried mine tailings. *Geochim Cosmochim Acta* 70, 2942–2956. <https://doi.org/10.1016/j.gca.2006.03.006>.
- Majzlan, J., Haase, P., Plášil, J., Dachs, E., 2019. Synthesis and stability of some members of the pharmacosiderite group, AFe<sub>4</sub>(OH)<sub>4</sub>(AsO<sub>4</sub>)<sub>3</sub>·nH<sub>2</sub>O (A = K, Na 0.5Ba, 0.5Sr). *Can Mineral* 57, 663–675. <https://doi.org/10.3749/canmin.1900035>.
- Bari, A.F., Lamb, D., Choppala, G., Seshadri, B., Islam, M., Sanderson, P., Rahman, M.M., 2021. Arsenic bioaccessibility and fractionation in abandoned mine soils from selected sites in New South Wales, Australia and human health risk assessment. *Ecotoxicol Environ Saf* 223, 112611. <https://doi.org/10.1016/j.ecoenv.2021.112611>.
- Liu, R., Kong, S., Shao, Y., Cai, D., Bai, B., Wie, X., Root, R.A., Gao, X., Li, C., Chorover, J., 2023. Mechanisms and health implications of toxicity increment from arsenate-containing iron minerals through in vitro gastrointestinal digestion. *Geoderma* 432, 116377. <https://doi.org/10.1016/j.geoderma.2023.116377>.
- Root, R.A., Chorover, J., 2023. Molecular speciation controls arsenic and lead bioaccessibility in fugitive dusts from sulfidic mine tailings. *Environ Sci Process Impacts* 25, 288. <https://doi.org/10.1039/d2em00182a>.

- [26] Ehlert, K., Mikutta, C., Jin, Y., Kretzschmar, R., 2018. Mineralogical controls on the bioaccessibility of arsenic in Fe(III)-As(V) coprecipitates. *Environ Sci Technol* 52, 616–627. <http://doi.org/10.1021/acs.est.7b05176>.
- [27] Mikutta, C., Mandaliev, P.N., Mahler, N., Kotsch, T., Kretzschmar, R., 2014. Bioaccessibility of arsenic in mining-impacted circumneutral river floodplain soils. *Environ Sci Technol* 48, 13468–13477. <https://doi.org/10.1021/es502635t>.
- [28] Sowers, T.D., Blackmon, M.D., Betts, A.R., Jerden, M.L., Scheckel, K.G., Bradham, K.D., 2023. Potassium jarosite seeding of soils decreases lead and arsenic bioaccessibility: A path toward concomitant remediation. *Proc Natl Acad Sci USA* 120, e2311564120. <https://doi.org/10.1073/pnas.2311564120>.
- [29] Ollson, C.J., Smith, E., Scheckel, K.G., Betts, A.R., Juhasz, A.L., 2016. Assessment of arsenic speciation and bioaccessibility in mine-impacted materials. *J Hazard Mater* 313, 130–137. <https://doi.org/10.1016/j.jhazmat.2016.03.090>.
- [30] Paktunc, D., Majzlan, J., Huang, A., Thibault, Y., Johnson, M.B., White, M.A., 2015. Synthesis, characterization, and thermodynamics of arsenates forming in the Ca-Fe(III)-As(V)-NO<sub>3</sub> system: Implications for the stability of Ca-Fe arsenates. *Am Mineral* 100, 1803–1820. <https://doi.org/10.2138/am-2015-5199>.
- [31] Yang, J.K., Barnett, M.O., Jardine, P.M., Basta, N.T., Casteel, S.W., 2002. Adsorption, sequestration, and bioaccessibility of As(V) in soils. *Environ Sci Technol* 36, 4562–4569. <https://doi.org/10.1021/es011507s>.
- [32] Meunier, L., Wragg, J., Koch, I., Reimer, K.J., 2010. Method variables affecting the bioaccessibility of arsenic in soil. *J Environ Sci A Tox Hazard Subst Environ Eng* 45, 517–526. <https://doi.org/10.1080/10934521003594863>.
- [33] Beak, D.G., Basta, N.T., Scheckel, K.G., Traina, S.J., 2006. Bioaccessibility of arsenic(V) bound to ferrihydrite using a simulated gastrointestinal system. *Environ Sci Technol* 40, 1364–1370. <https://doi.org/10.1021/es0516413>.
- [34] USEPA, 2017. Method 1340: In vitro bioaccessibility assay for lead in soil. US EPA Washington, DC. ([https://www.epa.gov/sites/default/files/2017-03/documents/method\\_1340\\_update\\_vi\\_final\\_3-22-17.pdf](https://www.epa.gov/sites/default/files/2017-03/documents/method_1340_update_vi_final_3-22-17.pdf)).
- [35] Bajda, T., 2010. Solubility of mimetite Pb<sub>5</sub>(AsO<sub>4</sub>)<sub>3</sub>Cl at 5–55°C. *Environ Chem* 7, 268–278. <https://doi.org/10.1016/j.gca.2011.01.021>.
- [36] Bohan, M.T., Mahoney, J.J., Demopoulos, G.P., Neelameggham, N.R., Alam, S., Oosterhof, H., Jha, A., Wang, S., 2014. Rare Metal Technology 2014. The Minerals, Metals & Material Society. John Wiley & Sons, New Jersey, pp. 9–11. <https://doi.org/10.1002/9781118888551.ch2>. The synthesis and stability of yukonite: Implications in solid arsenical waste storage.
- [37] Dutrizac, J.E., Jambor, J.L., 1988. The synthesis of crystalline scorodite, FeAsO<sub>4</sub>·2H<sub>2</sub>O. *Hydrometallurgy* 19, 377–384. [https://doi.org/10.1016/0304-386X\(88\)90042-4](https://doi.org/10.1016/0304-386X(88)90042-4).
- [38] Majzlan, J., Števkó, M., Plášil, J., Sejkora, J., Dachs, E., 2023. Thermodynamics of the Cu, Zn, and Cu-Zn phases: zincolivenite, adamite, olivenite, ludjibaite, strashimirite, and slavkovite. *J Geosci* 68, 67–80. <https://doi.org/10.3190/jgeosci.367>.
- [39] Villalobos, J., González-Flores, D., Urcuyo, R., Montero, M.L., Schuck, G., Beyer, P., Risch, M., 2021. Requirements for beneficial electrochemical restructuring: A model study on a cobalt Oxide in selected electrolytes. *Adv Energy Mater* 11, 2101737. <https://doi.org/10.1002/aenm.202101737>.
- [40] Wudarska, A., Sordyl, J., Manecki, M., Zawila, A., Bajda, T., 2022. Vibrational spectroscopic study of synthetic analogs of schultenite PbHAsO<sub>4</sub>–“phosphoschultenite” PbHPO<sub>4</sub> solid solution series. *Polyhedron* 211, 115534. <https://doi.org/10.1016/j.poly.2021.115534>.
- [41] Yuan, T.C., Jia, Y.F., Demopoulos, G.P., 2005. Synthesis and solubility of crystalline annabergite (Ni<sub>3</sub>(AsO<sub>4</sub>)<sub>2</sub>·8H<sub>2</sub>O). *Can Metall Quart* 44, 449–456. <https://doi.org/10.1179/cmq.2005.44.4.449>.
- [42] Filippi, M., Drahota, P., Machovič, V., Böhmová, V., Mihaljevič, M., 2015. Arsenic mineralogy and mobility in the arsenic-rich historical mine waste dump. *Sci Total Environ* 536, 713–728. <https://doi.org/10.1016/j.scitotenv.2015.07.113>.
- [43] Majzlan, J., Lazić, B., Armbruster, T., Johnson, M.B., White, M.A., Fisher, R.A., Plášil, J., Loun, J., Škoda, R., Novák, M., 2012. Crystal structure, thermodynamic properties, and paragenesis of bukovskýite, Fe<sub>2</sub>(AsO<sub>4</sub>)(SO<sub>4</sub>)(OH)·9H<sub>2</sub>O. *J Mineral Petrol Sci* 107, 133–148. <https://doi.org/10.2465/jmps.110930>.
- [44] Majzlan, J., Plášil, J., Dachs, E., Benisek, A., Mangold, S., Škoda, R., Abrosimova, N., 2021. Prediction and observation of formation of Ca–Mg arsenates in acidic and alkaline fluids: Thermodynamic properties and mineral assemblages at Jáchymov, Czech Republic and Rotgülden, Austria. *Chem Geol* 559, 119922. <https://doi.org/10.1016/j.chemgeo.2020.119922>.
- [45] Ruby, M.V., Lowney, Y.W., 2012. Selective soil particle adherence to hands: Implications for understanding oral exposure to soil contaminants. *Environ Sci Technol* 46, 12759–12771. <https://doi.org/10.1021/es302473>.
- [46] Schwertmann, U., 1964. Differenzierung der eisenoxide des bodens durch extraktion mit ammoniumoxalat lösung. *Z Pflanz Bodenkd* 105, 194–202.
- [47] Juhasz, A.L., Smith, E., Weber, J., Naidu, R., Rees, M., Rofe, A., Kuchel, T., Sansom, L., 2009. Assessment of four commonly employed in vitro arsenic bioaccessibility assays for predicting in vivo arsenic relative bioavailability in contaminated soils. *Environ Sci Technol* 43, 9887–9894. <https://doi.org/10.1021/es902427y>.
- [48] Malagelada, J.R., Lonstreth, G.G., Summerskill, W.H.J., Go, V.L.W., 1976. Measurement of gastric functions during digestion of ordinary solid meals in man. *Gastroenterology* 70, 203–210. [https://doi.org/10.1016/S0016-5085\(76\)80010-8](https://doi.org/10.1016/S0016-5085(76)80010-8).
- [49] Dodd, M., Lee, D., Nelson, J., Verenitch, S., Wilson, R., 2024. In vitro bioaccessibility round robin testing for arsenic and lead in standard reference materials and soil samples. *Integr Environ Assess Manag* 1–10. <https://doi.org/10.1002/ieam.4891>.
- [50] Huang, X., Chang, M., Han, L., Li, J., Li, S.H., Li, H.B., 2023. Variation of lead bioaccessibility in soil reference materials: Intra- and inter-laboratory assessments. *Chemosphere* 312, 137293. <https://doi.org/10.1016/j.chemosphere.2022.137293>.
- [51] Parkhurst, D.L., Appelo, C.A.J., 1999. User's guide to PHREEQC (Version 2): A computer program for speciation, batch-reaction, one-dimensional transport, and inverse geochemical calculations. U.S. Geological Survey, Water-Resource Investigations Report.
- [52] Carlson, L., Bigham, J.M., Schwertmann, U., Kyek, A., Wagner, F., 2002. Scavenging of As from acid mine drainage by schwertmannite and ferrihydrite: comparison with synthetic analogues. *Environ Sci Technol* 36, 1712–1719. <https://doi.org/10.1021/es0110271>.
- [53] Stubbe, P., Mikutta, C., Matulková, I., Drahota, P., 2024. Dissolved phosphate decreases the stability of amorphous ferric arsenate and nano-crystalline yukonite. *J Hazard Mater* 471, 134374. <https://doi.org/10.1016/j.jhazmat.2024.134374>.
- [54] Manning, B.A., Goldberg, S., 1997. Arsenic(III) and arsenic(V) adsorption on three California soils. *Soil Sci Soc* 162, 886–895. <https://doi.org/10.1097/00010694-199712000-00004>.
- [55] Smith, E., Naidu, R., Alston, A.M., 1999. Chemistry of arsenic in soils: I. Sorption of arsenate and arsenite by four Australian soils. *J Environ Qual* 28, 1719–1726. <https://doi.org/10.2134/jeq1999.00472425002800060005x>.
- [56] Ettlér, V., Čihlová, M., Jarošíková, A., Mihaljevič, M., Drahota, P., Kříbek, B., Vaněk, A., Penížek, V., Sracek, O., Klementová, M., Engel, Z., Kamona, F., Mapani, B., 2018. Oral bioaccessibility of metal(loid)s in dust materials from mining areas of northern Namibia. *Environ Int* 124, 205–215. <https://doi.org/10.1016/j.envint.2018.12.027>.
- [57] Jarošíková, A., Ettlér, V., Mihaljevič, M., Drahota, P., Culka, A., Racek, M., 2018. Characterization and pH-dependent environmental stability of arsenic trioxide-containing copper smelter dust. *J Environ Manag* 209, 71–80. <https://doi.org/10.1016/j.jenvman.2017.12.044>.
- [58] Yue, Z., Donahoe, R.J., 2009. Experimental simulation of soil contamination by arsenolite. *Appl Geochem* 24, 650–656. <https://doi.org/10.1016/j.apgeochem.2008.12.016>.
- [59] Magalhães, M.C.F., de Jesus, J.D.P., Williams, P.A., 1988. The chemistry of formation of some secondary arsenate minerals of Cu(II), Zn(II) and Pb(II). *Mineral Mag* 52, 679–690. <https://doi.org/10.1180/minmag.1988.052.368.12>.
- [60] Paktunc, D., Dutrizac, J., Gertsman, V., 2008. Synthesis and phase transformations involving scorodite, ferric arsenate and arsenical ferrihydrite: Implications for arsenic mobility. *Geochim Cosmochim Acta* 72, 2649–2672. <https://doi.org/10.1016/j.gca.2008.03.012>.
- [61] Djurdjević, P., 1990. The complexation between iron(III) ion and glycine in nitrate medium. *Transit Met Chem* 15, 345–350. <https://doi.org/10.1007/BF01177459>.
- [62] Marino, T., Toscano, M., Russo, N., Grand, A., 2006. Structural and electronic characterization of the complexes obtained by the interaction between bare and hydrated first-row transition-metal ions (Mn<sup>2+</sup>, Fe<sup>2+</sup>, Co<sup>2+</sup>, Ni<sup>2+</sup>, Cu<sup>2+</sup>, Zn<sup>2+</sup>) and glycine. *J Phys Chem B* 110, 24666–24673. <https://doi.org/10.1021/jp0645972>.
- [63] Basta, N.T., Foster, J.N., Dayton, E.A., Rodriguez, R.R., Casteel, S.W., 2007. The effect of dosing vehicle on arsenic bioaccessibility in smelter-contaminated soil. *J Environ Health Sci Part A* 42, 1275–1281. <https://doi.org/10.1080/10934520701434927>.
- [64] Rodriguez, R.R., Basta, N.T., Casteel, S.W., Armstrong, F.P., Ward, D.C., 2003. Chemical extraction methods to assess bioavailable arsenic in contaminated soil and solid media. *J Environ Qual* 32, 876–884. <https://doi.org/10.2134/jeq2003.8760>.